STAGNATION POINT RADIATIVE HEATING RELATIONS FOR VENUS ENTRY

Michael E. Tauber*, Grant E. Palmer**and Dinesh Prabhu**

ERC Corp., Huntsville, AL

Introduction

In December 1978, the United States landed four capsules on the surface of Venus. The Pioneer-Venus landers consisted of one large and three small probes that entered the atmosphere at various latitudes (Ref.1). In the intervening decades, no additional U. S. vehicles have landed on Venus, although there is active interest in future landing missions. The measurements of atmospheric composition and structure made by the Pioneer Venus probes during entry (Ref. 2) are of great value in refining the calculations of the heating that will be experienced by future probes. The objective here is to present improved analytic expressions for calculating the stagnation point radiative heating during entry into the atmosphere of Venus.

Simple, approximate expressions to calculate the stagnation point heating rates during atmospheric entries have been widely used for parametric mission studies and during the conceptual design of vehicles and probes. Because the resulting heating calculations require negligible computation time, they are incorporated in entry trajectory codes and can be used to calculate the approximate heat shield thicknesses at the stagnation point (Refs. 3 and 4). In turn, the stagnation point heat shield thickness can be used to estimate the mass of the forebody heat shield. Because the precise composition of the atmosphere was not well known during the design of the Pioneer Venus probes, the heating rates that were used to size the heat shields were calculated for an a volumetric mixture of 90% CO_2 and 10% N_2, (Ref. 5 and 6). The atmospheric composition, 96.5% CO_2 and 3.5% N_2 used in the present CFD calculations (Ref. 7) is that measured by the Pioneer-Venus large probe (Ref. 1). In addition, results from recent shock tube experiments and improved spectroscopic data for key molecular species are included in the calculations of radiative heating. The current, more precise results using Ref. 7 and 8 will be compared with the previous ones that were based on Ref. 5.

Analysis

The results presented in Ref. 5, among others, were used in the design of the Pioneer Venus probes and were obtained by solving the coupled thin shock-layer conservation equations for the non-gray radiative transport of a viscous, heat-conducting, emitting and absorbing gas in thermochemical equilibrium, thereby accounting for the non-adiabatic flow field of the radiating gas. Both radiative and convective heating rates *are tabulated in Ref. 5 as functions of flight velocities, stagnation pressure and shock

stand-off distance. However, for ease of application, the radiative heating rates were fitted with analytic expressions in terms of flight velocity, ambient atmospheric density and nose radius. The analytic expressions are valid for stagnation pressures from 1. to 10. atm, and nose radii from 0.20 to 0.75 m. The radiative heating rates from Ref. 5 are compared with results from two codes written at NASA Ames Research Center; these are the Data-Parallel Line Relaxation (DPLR) code (Ref. 7) and the Non-Equilibrium Air Radiation (NEQAIR) code (Ref. 8).

The DPLR code uses a modified Steger-Warming flux-splitting scheme that allows higher-order differencing of the inviscid fluxes without the excess numerical dissipation characteristic of standard flux splitting. The technique greatly accelerates convergence. For the Venus entry calculations presented here, a 16-species CO_2-N_2 gas mixture was used. The species considered were CO_2, CO, CO^+, C_2, N_2, O_2, NO, NO^+, CN, C, C^+, N, N^+, O, O^+ and e. Finite chemical reaction rates were used and a fully catalytic cold wall was assumed. (The effect of wall temperature was investigated and will be discussed.)

The NEQAIR code uses a line-by-line method to compute radiative emission and absorption spectra along a line-of-sight for atomic and molecular species, electronic band systems and infrared band systems. Individual electronic transitions are evaluated for atomic and molecular species. The code also models bound-bound and free-free continuum radiation caused by the interactions of electrons with neutral and ionized atomic species. The inputs to NEQAIR come from the DPLR code and consist of temperatures and species number densities along the stagnation line. Bound-bound (atomic line), bound-free, and free-free contributions were calculated from the atomic species, C, N, and O. The molecular vibrational band systems included in the computation were N_2 1+, N_2 2+, N_2 BH2, NO β, NO γ, NO δ, NO ε, O_2 SR, CN violet, CN red, CO (4+) and C_2 Swan. Results from recent computations of vibronic transition probabilities for the CO (4+), CN (violet and red) and C_2 (Swan) vibrational band systems were included. The population distributions in the excited states were calculated using a Boltzmann distribution. A tangent slab shock layer approximation was used to determine the radiative heating rate at the stagnation point.

The Pioneer-Venus measured atmospheric composition of 96.5% CO_2 and 3.5% N_2 was used in the calculations. Because the DPLR flow field and the NEQAIR radiative emission codes are uncoupled, the resultant radiative heating rates were corrected to account for the non-adiabatic nature of the flow field by using the relation (Eq. 1) that was derived in Ref. 9.

$$\frac{q_{rad}}{q_{rad.adiab}} = \frac{1}{1 + 3\Gamma^{0.7}} \qquad (1)$$

where

$$\Gamma = \frac{2q_{rad.adiab}}{0.5\rho_\infty v_\infty^3}$$

2

Although Eq. (1) was originally based on radiation from hydrogen and has been applied in air also (Ref. 10), it has been used here because no equivalent, more precise, expression is currently available for the Venus atmospheric gases. However, one possible justification for using Eq. (1) is the close agreement at peak radiative heating with the value based on Ref. 5 (to be shown below) since the energy equation used in Ref. 5 implicitly accounts for losses from radiative emission. At peak heating, the emission is primarily from atomic species and thus less sensitive to the initial molecular composition. (Although Ref.5 contains a comparison of adiabatic and nonadiabatic radiative heating at two flight conditions, neither point is representative of the Pioneer-Venus large probe's trajectory, in addition to being for a different atmospheric composition. Non-the-less, because the computational procedure used in Ref. 5 is similar to that employed in Ref. 11 for air, the two points for the 90% CO_2 + 10% N_2 atmosphere of Ref. 5 were compared with the equivalent conditions in air that are presented in Ref. 11.The results indicate that for the two flight conditions in Ref. 5, the ratio of nonadiabatic to adiabatic heating is 4 and 6% lower in the assumed Venus atmosphere of Ref. 5 than for air, as based on Ref. 11, Therefore, Eq. 1 may be somewhat conservative, based on the preceding comparison.)

The calculations were done for the Pioneer-Venus large probe using a nose radius of 0.363 m and a ballistic coefficient of 190. kg/m^2. The as-flown trajectory (Ref. 12) was computed using the Traj code (Ref. 4). The entry velocity and entry angle were11.584 km/s and -31.829 deg at an altitude of 137.78 km. The stagnation point radiative heating pulse was calculated using Eqs. (2a and 2 b) and is shown in Fig. 1. The equations are based on fits to 10 values of the more precise numerical calculations from Refs.7-9 in conjunction with the shock layer pressure and thickness dependence from Ref. 5.

For 10,028 m/s to 12,000 m/s

$$q_{rad} = 8.497x10^{-63} v_\infty^{18} \rho_\infty^{1.2} r_N^{0.49} \ \text{W/m}^2 \tag{2a}$$

For less than 10,028 m/s

$$q_{rad} = 2.195x10^{-22} v_\infty^{7.9} \rho_\infty^{1.2} r_N^{0.49} \qquad \text{W/m}^2 \tag{2b}$$

Note that all units are in the SI (mks) system and thus the radiative heating rate is in W/m^2 for consistency.

Results and Conclusions

The accuracy of the fitted equations is compared with the computed values in Table 1. A simple averaging of the 10 heating rates yields an absolute average accuracy

of 8%, but is skewed by the large disagreement at the first time point at 7 sec. (At t=7 sec, the stagnation pressure is a relatively low 0.36 atm and the heating rate is raised by the enhanced temperature from chemical non-equilibrium along the initial 40% of the stagnation line. At lower altitudes, the zone of chemical non-equilibrium shrinks rapidly as the shock layer pressure increases. For example, at the peak radiative heating time of 8.6 sec the stagnation pressure is 3.7 atm.) However, the contributions to the total radiative heating at the wings of the distribution are modest. Therefore, a more meaningful statistically weighed average difference is one arrived at by dividing each heating rate value by the peak rate, which yields an absolute average disagreement of only 2.5%.

Also shown in Fig. 1 for comparison, is the radiative heating pulse based on fits to the tabulated values in Ref. 5. (The heating rates in Ref. 5 were based on a wall temperature of 2500 K, whereas the present computations were for a cold wall. The influence of a 2500 K wall temperature on the present results was investigated. During the entry time interval from 7 to 8.8 sec when emission is dominated by atomic species, the hot wall radiative heating rate increased by an average of 0.4% and from 9.2 to 10.4 sec when the primary radiators are molecules, by 2.5%.) Note the close agreement in the peak rates, where about 90% of the emission is from atomic species. The significant secondary pulse predicted by Ref. 5 likely results from the excessive amount of radiative emission from molecular species, especially CN, due to the assumption of a 10% N_2 concentration in the early atmospheric model that was used in Ref. 5. As expected, the radiative heating contribution from CN (primarily at t>9.2 sec) is much less for the measured N_2 concentration of 3.5%. A comparison of the two stagnation point radiative heating pulses for the Pioneer Venus large probe (Fig. 1) shows that the present computations yield a 15% lower radiative heat load than the rates based on Ref. 5.

It is recommended that Eq. 2 be used in parametric mission studies, etc., in preference to similar expressions based on old calculations that assumed significantly higher atmospheric concentrations of N_2 than 3.5%. In addition, the present calculations were based on more accurate data for key molecular band systems and finite reaction rates. It is noteworthy, that during the descent from 92.22 km to 77.12 km (see Table 1), the Pioneer Venus large probe experienced stagnation point pressures from 0.81 atm to 10.0 atm, respectively. Therefore, Eq. 2 should give good results over a wide range of flight conditions at Venus.

Table 1. Stagnation point radiative heating rates of Pioneer Venus large probe; computed values compared with Eq. 2 results.

Time, sec	V, m/s	ρ, kg/m^3	Altitude, km	q_{rad}, W/cm^2	q_{rad}, Eq. 2, W/cm^2	% diff.
7.0	11551	2.86e-4	95.22	519	388	-25.2
7.5	11475	6.46e-4	92.22	936	915	-2.2
8.0	11310	1.39e-3	89.24	1672	1770	5.9
8.6	10880	3.26e-3	85.77	2449	2450	0.

8.8	10651	4.24e-3	84.65	2302	2288	-0.6
9.2	10028	6.92e-3	82.49	1396	1393	-0.2
9.5	9408	9.64e-3	80.98	1117	1252	12.1
9.7	8927	1.18e-2	80.02	990	1058	6.9
10.0	8134	1.55e-2	78.69	793	700	-11.7
10.4	7015	2.13e-2	77.12	374	318	-15.
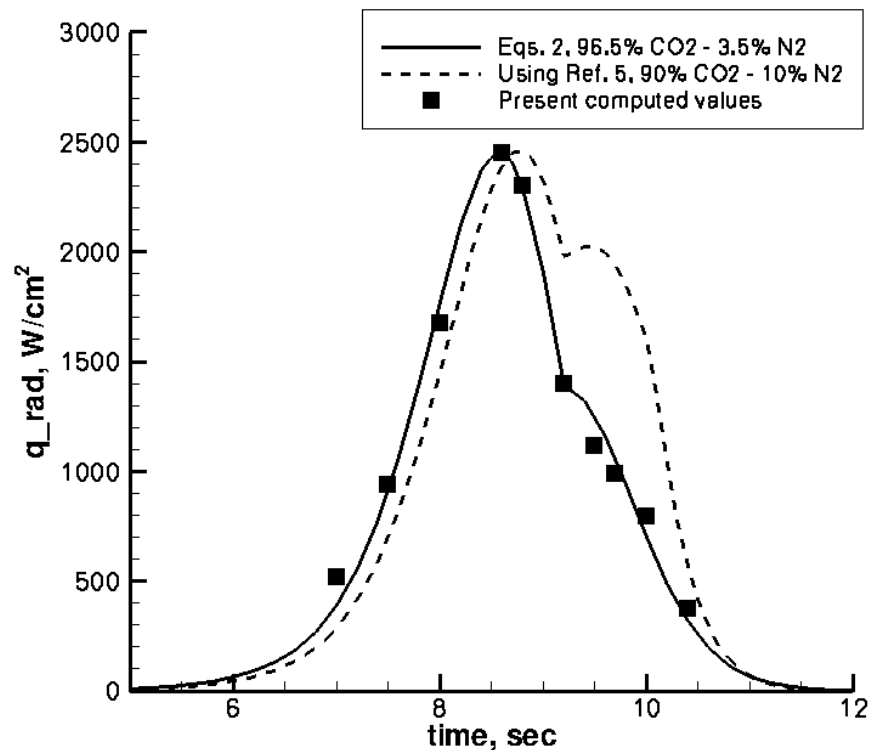
Figure 1. Comparison of stagnation point radiative heating rates for Pioneer-Venus large probe using Eq. 2 and computed points and outdated rates from Ref. 5

ACKNOWLEDGEMENT

REFERENCES

1. Fimmel, R. O., Colin, L. and Burgess, E., "Pioneer Venus", NASA SP-461, 1983.

2. Seiff, A. and Kirk, D. B., "Structure of the Venus Mesosphere and Lower Thermosphere from Measurements during Entry of the Pioneer Venus Probes", ICARUS, Vol. 49, 1982, pp. 49-70.

3. Tauber, M. E. and Sutton, K., "Stagnation Point Heating Relations for Earth and Mars Entries", Journal of Spacecraft and Rockets, Vol. 28, No. 1, Jan.-Feb. 1991, pp.40-42.

4. Allen, G. A., Jr., Wright, M. J. and Gage, P., "The Trajectory Program (Traj) Reference Manual and User's Guide", NASA TM-2004-212847, 2005.

5. Page, W. A. and Woodward, H. T., "Radiative and Convective Heating During Venus Entry", AIAA Journal, Vol. 10, No. 10, Oct. 1972, pp.1379-1381.

6. Sutton, K.. "Characteristics of Coupled Non-Gray Radiating Gas Flows with Ablation Product Effects About Blunt Bodies During Planetary Entry", Ph.D. Dissertation, North Carolina State University, Raleigh, NC, 1973.

7. Wright, M. J.,White, T. and Mangini, N., "Data-Parallel Line Relaxation Methods (DPLR) Code User Manual Acadia-Version 4.01.1", NASA/TM-2009-215388, Oct. 2009.

8. Whiting, E. E., Park, C., Liu, Y., Arnold, J. O. and Paterson, J., "NEQAIR96 Nonequilibrium and Equilibrium Radiative Transport and Spectra Program: User's Manual", NASA RP-1389, December 1996.

9. Tauber, M. E. and Wakefield, R. M., "Heating Environment and Protection During Jupiter Entry", Journal of Spacecraft and Rockets, Vol.8, No. 6, June 1971, pp. 630-636.

10. Prabhu, D., Saunders, D., Liu, Y., Hash, D. and Dateo, C., "Preliminary Estimates of Radiative Heating for the CEV Heatshield", NASA CAP TN/EG-CEV-06-8, Jan. 2006.

11. Page, W., Compton, D., Borucki, W., Ciffone, D. and Cooper, D., "Radiative Transport in Inviscid Nonadiabatic Stagnation Region Shock Layers", AIAA Paper No. 68-784, Los Angeles, CA, June 1968. Also "Progress in Astronautics & Aeronautics", Academic Press Inc., New York, NY, 1969, pp. 75-114.

12. Seiff, A., Kirk, D. B., Young, R. E., Blanchard, R. C., Findlay, J.T., Kelly, G.M. and Sommer, S.C., "Measurements of Thermal Structure and Thermal Contrasts in the Atmosphere of Venus and Related Dynamical Observations: Results from the Four Pioneer Venus Probes", Journal of Geophysical Research, Vol. 85, No. A13, December 30, 1980, pp.7903-7933.